Omega-P, Inc.
199 Whitney Avenue, Suite 200
New Haven, CT 06511

Final Report to US Department of Energy

on

Phase I SBIR Grant DE-FG02-04ER84031

QUASI-OPTICAL 3-dB HYBRID FOR FUTURE HIGH-ENERGY ACCELERATORS

Principal Investigator: J. L. Hirshfield
December, 2005

TABLE OF CONTENTS

1. IDENTIFICATION AND SIGNIFICANCE OF THE PROBLEM, AND TECHNICAL APPROACH

1a. Introduction

Under Topic 6b in the 2004 DoE SBIR Program Solicitation, entitled *Radio Frequency Power for Linear Colliders,* grant applications were sought for high-power rf circulators, isolators, switches, quasi-optical components, and high-power rf pulse compression methods, for use in future linear colliders. These components—amongst others that are also sought—must be capable of operation at high pulse powers (20-100 MW), at high frequencies (11-40 GHz), and for pulse lengths of several microseconds. In response, Omega-P, Inc. proposed and was awarded the Phase I grant DE-FG02-04ER-84031 "Quasi-Optical 3-dB Hybrid for Future High-Energy Accelerators." This project aimed to apply quasi-optical concepts for development of two related components. One component is an isolator, for preventing power that is unavoidably reflected from a pair of resonant (standing-wave mode) accelerator sections from returning to the rf amplifiers. The second component is a four-port switch (often referred in the Russian literature as a "combiner-commutator") for selectively directing rf power combined from two sources into one or another outgoing port. This switch could play a central role in a DLDS-like arrangement for combining, at a sequence of local junctions, the longer pulse outputs of several rf sources into a single pulse of shorter duration and greater peak power for driving a set of accelerator sections. For convenience, we refer to these components together as variants of a "magic-Y," with deference to the classical *magic-T* single-mode rectangular waveguide element.

The effort during Phase I, and that proposed for Phase II, was primarily for components to operate at 34.272 GHz, the frequency of the newly-commissioned Omega-P magnicon amplifier. This tube—although only partially-conditioned—is already supplying >10 MW, >0.25 μs pulses, and is the highest-power accelerator-class mm-wave amplifier in operation. In addition, a full complement of 34-GHz high-power over-moded (or quasi-optical) high-power windows and transmission-line components that are already developed are available for testing of the new components described here. Furthermore, a 34-GHz quasi-optical resonant ring and a 34-GHz passive rf pulse compressor ("QO SLED") are also under development by Omega-P, either of which could be used to test the components at multiples of the peak power of 45 MW that is expected to be available from the 34-GHz magnicon. This accumulation of 34-GHz high-power rf technology was developed recently by Omega-P, with support under several Phase I and Phase II DoE SBIR grants, for establishment of a test bed for high-field breakdown studies, millimeter-wave component development, and advanced high-gradient accelerator prototypes.

The need for this test bed (to a number of scientists in the field) is actually heightened by the recent decision* to select superconducting RF technology for the International Linear Collider ILC. This heightened need is because the acceleration gradient limit of 25-35 MeV/m in niobium superconducting cavities makes it impractical to achieve a center-of-mass energy greater than about 800 GeV within a reasonable geographical footprint. For higher center-of-mass energy, a higher acceleration gradient is required; thus the need for basic studies at cm- and mm-wavelengths where preliminary tests at SLAC, KEK, and CERN show that gradients >100 MeV/m may indeed be practical in room temperature structures. But to reach this goal, test facilities must be built and sustained; the present proposal is for development of a pair of components that could add considerable flexibility to the capabilities of such a test facility.

*Final report of ITRP, submitted to ILCSC and ICFA, September 2004.

While the principal efforts in this work were for development of 34-GHz quasi-optical components, the basic principles underlying the magic-Y interaction can be exploited at frequencies other than 34 GHz. During Phase I, in addition to 34-GHz devices, designs for 11.424 GHz were also worked out. Furthermore, the magic-Y can be also scaled to operate much higher than 34 GHz, should future interest arise. During Phase II, focus would have been on realizing a Magic-Y and testing it with the multi-megawatt 34 GHz Omega-P magnicon [8]. The Phase II grant for this project was not approved.

1b. Technical Approach

1b.1. Quasi-optical 3-dB hybrid junction: Magic-Y.

Any grating is known to scatter an incident plane wave into several mutually phase-coherent secondary waves; the reciprocal process gives wave combining. The grating can take the form of a metal corrugated surface splitting an incident wave into mirror and anti-mirror waves of equal amplitudes, as illustrated in Fig. 1a. In the reciprocal case, shown in Fig. 1b, the combined wave beam direction is changed by means of ±90º mutual phase shifts between the input beams. This property of gratings is used in the quasi-optical components described below.

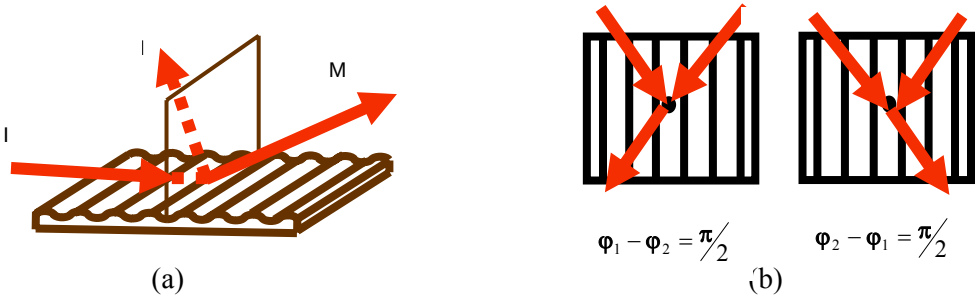

Fig. 1. Magic-Y: a quasi-optical 3-dB hybrid.
Fig. 1a shows a wave splitter, while Fig. 1b shows a wave combiner.

1b.2. Magic-Y as a phase-controlled binary beam combiner-commutator.

A grating working as a 3-dB hybrid coupler can be configured into a phase-controlled wave beam combiner-commutator that could be used in a quasi-optical version of DLDS. The topology of this device is shown in Fig. 2, where rf powers from eight sources are directed sequentially to accelerator sections by appropriate phase control of the sources.

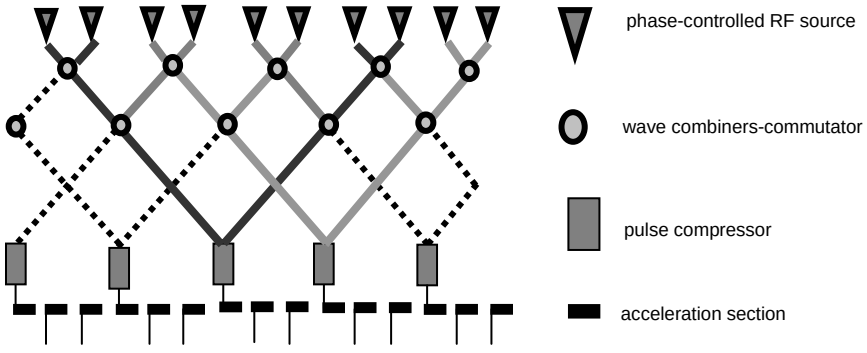

Fig. 2. Topology of a phased array feed for sequential combining of power from eight sources to drive sets of three accelerator sections.

1b.3. Magic-Y as an isolator.

To protect high power microwave amplifiers from unavoidable reflections of power incident upon resonant accelerating sections (as in standing-wave-mode accelerator operation), a scheme based on the quasi-optical 3-dB hybrid can be used. A schematic of the idea is illustrated in Fig. 3. An rf pulse compressed by a quasi-optical SLED is divided into two beams by the magic-Y which feed two identical accelerating sections. Reflected waves incident back onto the magic-Y are combined, diffracted into another direction, and absorbed by a dummy load, thereby preventing reflected power from returning to the source.

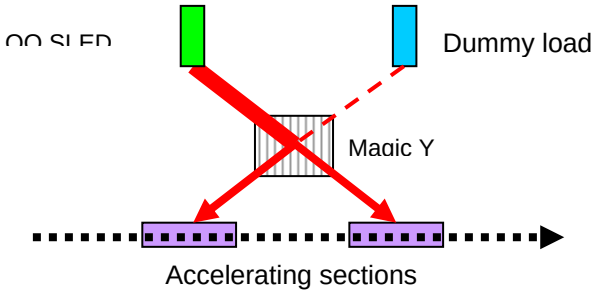

Fig. 3. Magic-Y isolator: non-reflection feed to accelerating sections, as in a 3-dB hybrid.

Gaussian wave beams are a promising option for long-line, low-loss transmission of high RF powers, as used in numerous radar systems, rf plasma heating complexes, and technological RF heating setups [15]. Such beams are transmitted by mirror lines or corrugated waveguides (as shown in Fig. 4). These are very convenient for introducing bends and junctions between sections. The main advantage of such systems is that the high power transmission capacity is combined with efficient mode filtration. For instance, the main HE_{11} (hybrid, quasi-Gaussian) mode of circular-cross-section corrugated waveguide (see Fig. 4b) has a very low field at the

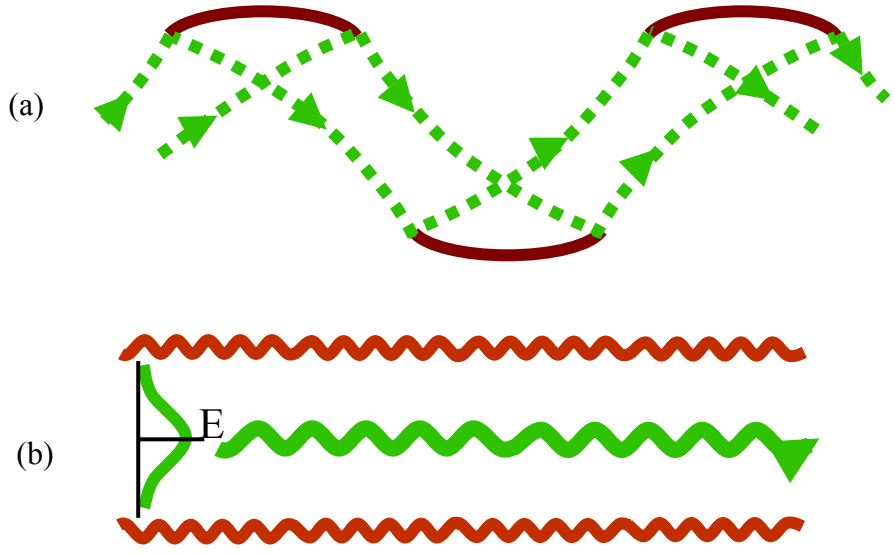

Fig. 4. Two examples of oversized waveguides for low-loss, pure mode transmission of (quasi-) Gaussian beams. (a) mirror line; (b) corrugated oversized waveguide.
Either of these concepts could be employed in a cm-wavelength magic-Y isolator.

waveguide surface, whereas spurious modes have much higher fields at the surface, and thus undergo much stronger absorption. In some cases corrugated waveguides are intentionally made of lossy materials (e.g. stainless steel) which allows one to avoid using special distributed absorbers, as would be required for closed systems using purely cylindrical smooth waveguide sections. Techniques for fabricating oversized corrugated waveguide and employing them in high-power installations for plasma heating are well established.

2. ANTICIPATED PUBLIC BENEFITS

Benefits to the US scientific community and to the public at large can be anticipated from results of future basic research in elementary particle physics, as has been amply demonstrated from such research in the past. The specific justification for efforts to develop microwave technology at frequencies of 11.424 GHz and higher for a future electron-positron collider rests principally on the anticipated scaling of acceleration gradient with frequency, which is nearly linear. Thus, the unloaded acceleration gradient for NLC was expected to be 73.4 MV/m, about four times that of SLC which operated at 2.856 GHz. By the same token, extrapolation by another factor-of-three in frequency would suggest that unloaded gradients exceeding 200 MV/m could be obtained by operating at 34.272 GHz. Technical achievement of high-gradient mm-wave linacs would carry distinct benefits to science and society of lower cost and smaller geographical footprint. This potential benefit assumed increased relevance, in light of the recent decision to build the forthcoming linear collider ILC based on superconducting RF technology, since the ultimate center-of-mass energy that this choice implies cannot be greater than about 0.8 TeV. To meet a future demand for a collider with multi-TeV capability, a different technology is required. Thus the need to further advance understanding of the potential for high-gradient acceleration using cm- and mm-wave sources and structures. The near-term technical benefit of the quasi-optical RF isolator and combiner-commutator development program proposed here is to demonstrate that a means will exist for transporting and directing the multi-100 MW peak power rf pulses that are needed for such studies. The long-term benefit could be to make possible construction of a high-gradient test accelerator which—if successful—could allow practical realization of a multi-TeV-scale electron-positron collider.

But also in the near-term, extensions of the millimeter-wave concepts to the centimeter-wave regime, namely to 11.424 GHz where NLC was proposed, could allow tests of a quasi-optical 3-dB hybrid four-port junction for isolating high-power klystrons from the resonant microwave circuits that follow, be they dual delay-line SLED-II rf pulse compressors, or accelerator structures themselves. Reflections from such resonant structures are endemic, and a means is desired for diverting the reflected energy to a dummy load, rather than to the klystron itself. This need is difficult—if not impossible—to satisfy using a traditional circulator or isolator that rests upon the non-reciprocal properties of waves that propagate in ferrites, since designs have not yet been found for handling the high peak and average rf powers. The project proposed here has the potential to remedy this problem, by providing an all-metallic structure that can provide high-power transport and diversion of rf energy in a future collider.

3. DEGREE TO WHICH PHASE I DEMONSTRATED TECHNICAL FEASIBILITY

In the following four sub-sections, results of the Phase I study are summarized. As shall be shown, these preliminary results provide strengthened confidence in the concepts propounded in the Phase I proposal, and form the basis for design, fabrication, and high-power testing in Phase II of structures that incorporate the Magic-Y.

3a. Theory of phase-controlled grating-based wave beam combiner-commutator

First, some new theoretical analysis is presented which is needed for design of realistic components. It is shown below, for the binary wave beam combiner-commutator representing a metallic diffraction grating [1], that the power loss is inverse proportional to the beam cross-section and that the frequency bandwidth is inverse proportional to the beam width.

One of methods to feed linear electron accelerators is based on using a delay line distribution system (DLDS) composed of phase-controlled binary wave combiners-commutators [2]. At millimeter wavelengths [3], such elements must be, obviously, of a quasi-optical type. One of such elements—the magic Y [1]—is based on the diffraction of plane wave by metallic grating. The number of scattered waves (diffraction maxima) is known to depend on the grating period [4, 5]. A proper choice of the primary wave incidence angle and the corrugation period provides only two scattered waves: the mirror beam and the minus-first-order beam. In such a case, projections of the incident $\vec{k}_{in}$ and the minus-first-order $\vec{k}_{-1}$ wave propagation vectors in the (x,y) plane (perpendicular to corrugation grooves) can be made counter-directional (Fig. 5); this is valid under the conditions $\pi/d = k_{y,in}$ and $\tan\left|k_{y,in}/k_{x,in}\right| > \sqrt{2}/4$.

Let all the wave structure be E-polarized ($H_z = 0$) that is favorable for raising the RF breakdown threshold. At a proper corrugation amplitude h, the mirror and anti-mirror scattered waves are of equal power densities. In this case, the inverse propagation of waves gives combining of two waves into one. In the resulting wave combiner (Fig. 6), the output wave propagation direction depends on the mutual phases between incident waves [1].

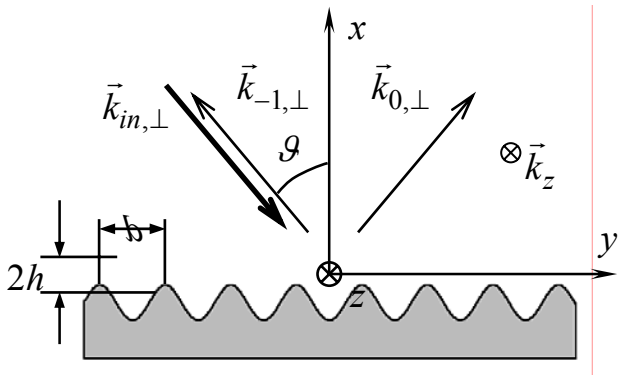

Fig. 5. Plane wave diffraction: projections of wave propagation vectors on the (x, y) plane perpendicular to the corrugation grooves.

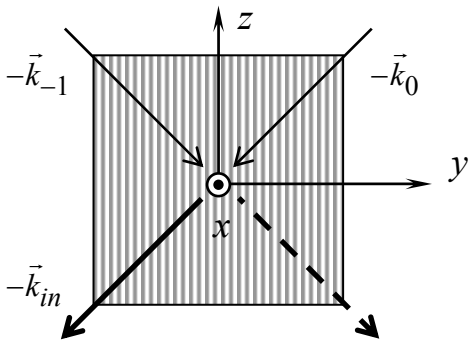

Fig. 6. The wave combiner-commutator "Magic Y", viewed in a direction perpendicular to the grating.

In a real situation, the incident wave beam is of a finite-cross-section and, so, represents a continuous paraxial set of plane waves

$$E_{z,in}(\vec{r}) = \int_{-\infty}^{\infty}\int_{-\infty}^{\infty} \tilde{E}_{z,in}(\vec{\kappa})\cdot\exp\left(i\vec{K}_{in}(\vec{\kappa})\cdot\vec{r}\right)d^2\vec{\kappa}\,, \qquad (1)$$

where $\vec{\kappa}$ is the projection of the wave propagation vector onto the plane perpendicular to the beam propagation direction; for definiteness, all the waves are assumed E-polarized ($H_z = 0$). For each partial incident plane wave, the scattered waves can be found numerically basing on solution of the two-dimensional scalar problem. The complex scattering coefficients $R_n(\vec{\kappa}) = A_n(\vec{\kappa})\exp(i\psi_n(\vec{\kappa}))$ can be linear approximated

$$R_n(\vec{\kappa}) \approx R_n(0) + \left(\frac{\partial R_n}{\partial K_\perp}\frac{dK_\perp}{d\vec{\kappa}} + \frac{\partial R_n}{\partial\theta}\frac{d\theta}{d\vec{\kappa}}\right)\Bigg|_{\vec{\kappa}=0}\cdot\vec{\kappa}\,,$$

where n=0,–1 is the order of the diffraction maximum, $K_\perp\left(\vec{\kappa}=0\right) = k_\perp$, $\theta(\vec{\kappa}=0) = \vartheta$. Vectors $\vec{K}_n\left(\vec{\kappa}\right)$ are related to $\vec{K}_{in}\left(\vec{\kappa}\right)$ by formulas

$$K_{n,y} = K_{in,y} + \frac{2\pi}{d}n\,,\ K_{n,z} = K_{in,z}\,,\ \left|\vec{K}_n\right|^2 = \left|\vec{K}_{in}\right|^2 = \left|\vec{k}_{in}\right|^2, \qquad (2)$$

that can be approximated by up to second order expansions in κ/k. Having calculated each partial scattered wave, we find the reflected beams in the form of integrals

$$E_{z,n}(\vec{r}) = \int_{-\infty}^{\infty}\int_{-\infty}^{\infty} \tilde{E}_{z,in}(\vec{\kappa})\cdot R_n\left(\vec{\kappa}\right)\cdot\exp\left(i\vec{K}_n(\vec{\kappa})\cdot\vec{r}\right)d^2\vec{\kappa}\,.$$

For the sake of symmetry and convenience, it can be assumed that the magic-Y is fed with a Gaussian wave beam of elliptic cross-section so that it illuminates a circular area at the grating and has a flat phase front approaching it. At $d\psi_n/d\vec{\kappa} \neq 0$, locations of the reflected beams will be determined by the Guss-Henken effect [5]. Obviously, they will not be pure Gaussian. The causes of their deformation in the lower infinitesimal order of inverse beam width $\lambda/a_\perp$ are the linear part of the dependence A_n upon $\vec{\kappa}$ and features of the wave vector transformation under (–1)-st order diffraction. Deformations arising from the first cause can be excluded, and from the second can be minimized, having accepted, that the reflected beams have

a deflection of the propagation direction from that appropriate for plane waves. In view of this, the loss in the non-Gaussian part of the mirror beam is of the order of $(\lambda/a_\perp)^4$, and for the anti-mirror beam of the order $(\lambda/a_\perp)^2$. Below some results for a beam with a greater half-width at the e^{-1} intensity level equal to a are listed. The displacements of a mirror beam perpendicular and parallel to the reflection plane are

$$\Delta_{0,\perp} = \frac{k_z}{k_\perp\sqrt{k^2-k_x^2}}\left(\frac{\partial\psi_0}{\partial\vartheta}\frac{k_x}{k_\perp} - \frac{\partial\psi_0}{\partial k_\perp}k_y\right),$$

$$\Delta_{0,\|} = \frac{k_x}{k_\perp\sqrt{k^2-k_x^2}}\left(\frac{\partial\psi_0}{\partial\vartheta}\frac{k_y k}{k_x k_\perp} + \frac{\partial\psi_0}{\partial k_\perp}\frac{k_z^2}{k}\right).$$

Angle of deflection of an anti-mirror beam in the reflection plane is

$$\varphi_{-1,\|} = \frac{k_z^2}{A_{-1}k_x^2 k_\perp a^2\sqrt{k^2-k_x^2}}\left(\frac{\partial A_{-1}}{\partial\vartheta}\frac{k_y\left(k^2-2k_z^2\right)}{k_z^2 k_\perp} - \frac{\partial A_{-1}}{\partial k_\perp}k_x\right) - \frac{k_y^2\sqrt{k^2-k_x^2}}{2k_x^3k^2a^2}.$$

Here the second term that is independent of A_{-1} results from the specific dependence of the non-mirror wave propagation direction on the direction of the incident wave. The displacements and angular deflections of the beam that results from an in-phase combining of mirror and anti-mirror beams from different sources, are sums of the half-values of each of the reflected beams apart, and the relative power of the non-Gaussian content is four times smaller, than that of the (–1)-st beam.

In the magic-Y, there are three kinds of diffractional power losses, namely filtration loss, polarization loss, and commutation loss. Filtration loss arises if on the input and output of the combiner-commutator there are directions, transporting Gaussian beams and filtering out all other modes, because of the non-Gaussian content of a total beam. Polarization loss arises since linearly polarized Gaussian beams differs from E-polarized Gaussian beams (1) by containing an H-component whose relative magnitude is $k_z^2/2k_x^2k^2a^2$. So the use of beams with $H_z \neq 0$ will result in additional loss. Commutation loss arises in switching by changing relative phases to redirect the total power into either of the two possible outputs. For example, let suppose that as a result of two beams of equal powers combining there is only one reflected Gaussian beam. If the phase of one of the incident beams is shifted by π then the basic part of power will go in a direction alternative to the previous one, but there will be reflected wave going in the former direction with relative parasitic power

$$\frac{\delta P_c}{P_\Sigma} = \frac{4k_z^2}{k_\perp^2a^2\left(k^2-k_x^2\right)}\left(\left(\frac{\partial A_0}{\partial\vartheta}\frac{k_x}{k_\perp} - \frac{\partial A_0}{\partial k_\perp}k_y\right)^2 + \left(\frac{\partial A_0}{\partial\vartheta}\frac{k_y k^2}{k_x k_z k_\perp} + \frac{\partial A_0}{\partial k_\perp}k_z\right)^2\right).$$

All three kinds of power losses are of the same order, namely $(ka)^{-2}$, diminishing as the area of the beams increases.

It is also necessary to consider the frequency bandwidth of the magic-Y, which in the above analysis was optimized for a fixed frequency. Obviously, the frequency deviation from the design value will result in additional loss. The effect caused by the deflection of the (–1)-st beam can be described within the framework of geometrical optics. The corresponding frequency half-bandwidth

$$\frac{\Delta\omega}{\omega} = \frac{k^2}{k_y a}\sqrt{\frac{k^2 - k_x^2}{2\left(k_x^4 k_y^2 + k^4 k_z^2\right)}},$$

is inverse proportional to the wave beam width a.

As an example, for the combiner-commutator based on using a grating with sinusoidal corrugation, where beam propagation directions are to form identical angles with the main axes of symmetry, the above analysis allows one to calculate that the corrugation period and amplitude should be $d = 0.866 \cdot \lambda$ and $h \approx 0.35 \cdot \lambda$. The non-Gaussian content of an anti-mirror beam ($\delta P_{-1}/P_{-1}$), the commutation loss ($\delta P_c/P_\Sigma$), and the frequency half-bandwidth ($\Delta\omega$) are

$$\frac{\delta P_{-1}}{P_{-1}} \approx 0.06 \cdot \frac{\lambda^2}{a^2},\ \frac{\delta P_c}{P_\Sigma} \approx 0.14 \cdot \frac{\lambda^2}{a^2},\ \frac{\Delta\omega}{\omega} = 0.26 \cdot \frac{\lambda}{a}.$$

These results were used for designing the devices described in the following sections.

3b. Experiment with a low-power, non-vacuum 34 GHz Magic-Y

An experimental 34 GHz magic-Y was built to test the basic concepts embodied in the analysis outlined above. The low-power, non-vacuum device was built in a symmetric configuration, where the incident and reflected beams made equal angles with all basic directions imposed by the grating; every beam had an 35.3º angle relative to the grating plane. The illuminated area at the grating plane was circular. Accordingly, all wave beams were of elliptic Gaussian cross-section and had flat phase fronts at the grating. The waves were *E*-polarized relative to the grove direction, which is favorable for withstanding high powers. The beam width was chosen to be large enough to limit to within ~1 % distortions due to the dispersion of elementary plane waves comprising the beams, but small enough to mitigate tolerances on mirror angular positioning.

The most obvious scheme to test the magic-Y would include an rf source, a beam splitter, a phase shifter and, after the magic-Y, two receivers, as diagrammed in Fig. 7. But in the experiment that was carried out, the more convenient scheme shown in Fig. 8 was used, that included only one receiver-detector.

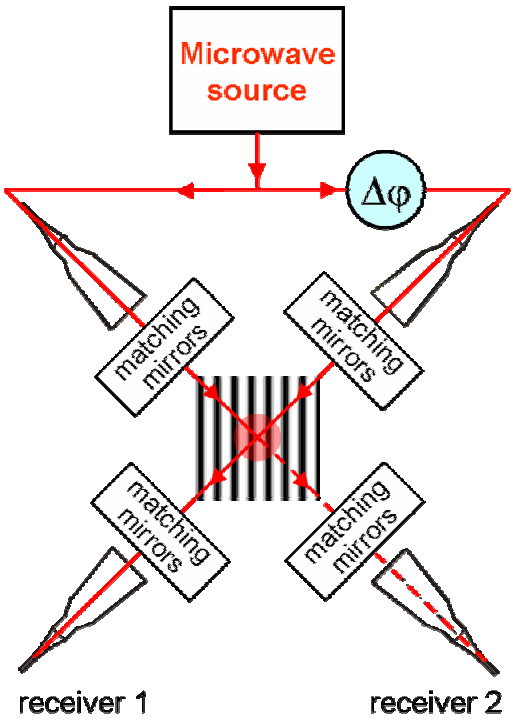

Fig. 7. The obvious scheme to test the Magic Y.

To provide the mutual coherence of quasi-optical beams incident to and scattered by the grating, a microwave source common for all beams was used. The beam splitting and combining was performed by the same grating.

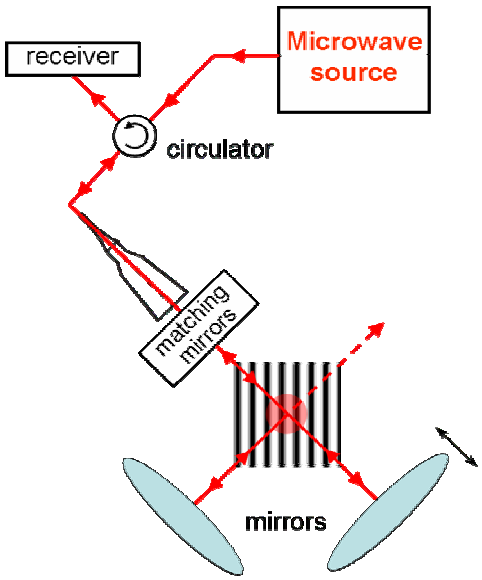

Fig. 8. The practically used scheme to test the magic-Y.

The experimental set-up is pictured in Fig. 9 and has parameters listed in Table I. The elements of the set-up include: *1* – a transmit-receive transducer that matches the TE_{10} mode of standard WR-28 rectangular waveguide to a Gaussian beam at the aperture of a 60 mm diameter horn; *2* – a focusing mirror of 300×271 mm^2 size (here and below the first size refers to the horizontal plane), the mirror surface being a paraboloid of revolution with a radius of curvature of 940 mm; *3* – a focusing mirror of 225×272 mm^2 size, the mirror surface being a parabolic cylinder of 1934 mm radius of curvature in the vertical plane; *4* – a flat grating of 180×180 mm^2 size, with a sinusoidal corrugation having a 7.58 mm period and a 3.05 mm amplitude; *5a*, *5b* – identical focusing mirrors of 225×260 mm^2 size, the mirror surface being an elliptic paraboloid with radii of curvature of 1850 and 823 mm. Distances between optical centers of these objects were: between *1* and *2* - 534 mm; between *2* and *3* – 379 mm; and between *4* and *3*, *5a*, *5b* – 694 mm.

Table I. Parameters of the 34-GHz experimental set-up.

Object number	Transverse sizes (mm)	Radii of curvature (mm)	Distances between objects (mm)
1 (horn)	60×60		534
2	300×271	940×940	379
3	225×272	∞×1934	694
4 (grating)	180×180	∞×∞	694
5a, ***5b***	225×260	1850×823	

The first size is in the horizontal plane.

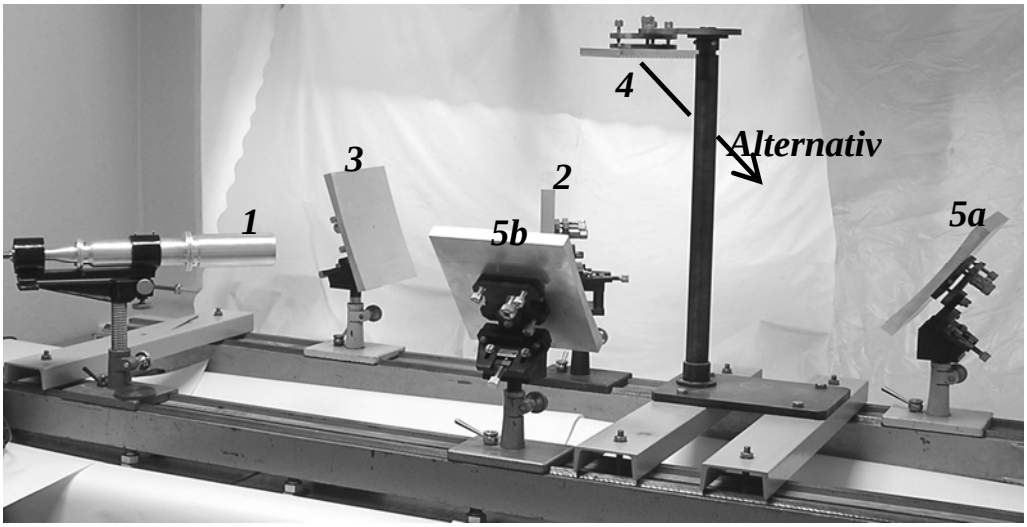

Fig. 9. A photo of the experimental set-up. Figures specify numbers of objects in the sequence of beam path-tracing. The arrow marks the direction of the alternative radiation.

The axisymmetric beam from the horn transformed by mirrors *2* and *3* into the elliptical one, is divided by the grating into two identical beams directed to mirrors *5a* and *5b*; having been reflected by the mirrors, the beams return back to the grating and are combined by it. The phase shift between the returned beams is determined by the difference between arms *4–5a* and *4–5b*. By moving a mirror *5a* or *5b* counter the incident beam, it is possible to distribute the rf power between the beam returning back to the horn and the beam leaving in the alternative direction (Fig. 7). The set-up (Fig. 8) included a klystron microwave generator modulated by rectangular video-pulses, a high-precision waveguide attenuator, a circulator, the magic-Y with wave matching system (Fig. 9), a microwave detector and a digital oscilloscope.

Fig. 10 shows data for the power returned back into the horn as a function of the normal displacement of the mirror *5a* (Fig. 9). The maximum returned power was more than 92% of the incident power. That corresponds to the loss in a single passage of about 4%. The minimum power returned back into the horn (when most of the power was radiated in the alternative direction, (Fig. 9) did not exceed 0.25 %. Within the measurement accuracy, the curve shown in Fig. 10 has a period equal to one half-wavelength, as anticipated from elementary considerations.

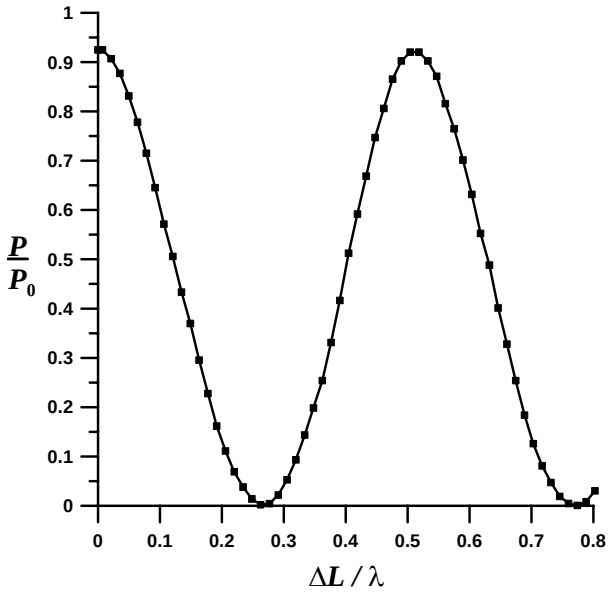

Fig. 10. Experimental curve for the power returned back to the horn as a function of mirror 5*a* displacement.

When between the grating and one of the mirrors *5a* or *5b* a plate was inserted that reflected the beam aside, the relative power returned to the horn was about 23%. After replacement of the grating by a flat mirror with an arbitrary positioning of the reflecting mirrors, about 94.5% of the power returned back to the horn. These findings indicate that the total two-pass loss due to the grating was about 2.5%. Thus, after subtracting out the losses in the transmitting matching system, the efficiency of the magic-Y itself was found to be about 96%.

These experimental results confirm the theoretical design considerations for this class of quasi-optical components, and provide a firm basis for further development during Phase II of a high-power, high-vacuum prototype of the magic-Y for test and evaluation at 34.272 GHz.

3c. Conceptual design of an 11.4 GHz 3-dB quasi-optical hybrid

In this section, an experimental set-up that could be used for testing an 11.4 GHz wave beam combiner-commutator is described. The 3-dB hybrid is assumed to be of the plane configuration, as diagrammed in Fig. 3. For the computer simulations, waveguides were taken to be circular corrugated, and their diameters were taken equal to five free-space wavelengths; axes of all waveguides were oriented in a common plane (planar configuration). The HE_{11} (quasi-Gaussian) modes radiated from the waveguides were taken to be *E*-polarized relative to the grating. The corrugation was sinusoidal with period of 23.47 mm and an amplitude of 5.43 mm.

In the 3-dB planar configuration hybrid, the diffraction grating divides an initial beam into two beams of different cross-sections that dictate positions and parameters of the matching mirrors. An example of this is depicted in Fig. 11, and parameters are listed in Tables II-IV.

Table II. Parameters of mirrors.

mirror element	dimensions (mm^2)	radii of curvature (mm^2)
M1	503×449	1173×932
M2	566×457	3448×2375
M3	362×369	1452×1163
Grating	584×343	∞×∞

Table III. Distances between centers of objects.

first element	second element	distance (mm)
M1	grating	960
M2	grating	960
waveguide (input 1, output 1)	M1	616
M3	M2	979
waveguide (input 2, output 2)	M3	480

Table IV. Angles.

first element	second element	third element	angle (deg)
M2	grating	M2	36
M1	grating	M1	108
waveguide (input 1, output 1)	M1	grating	54
grating	M2	M3	22
waveguide (input 2, output 2)	M3	M2	22

As is seen, the dimensions of this structure are considerable, and may well mitigate against its practicality. For this reason, it is more than likely that reduction to practice of the magic-Y concept at X-band during Phase II will follow lines outlined in Section 3b.3.

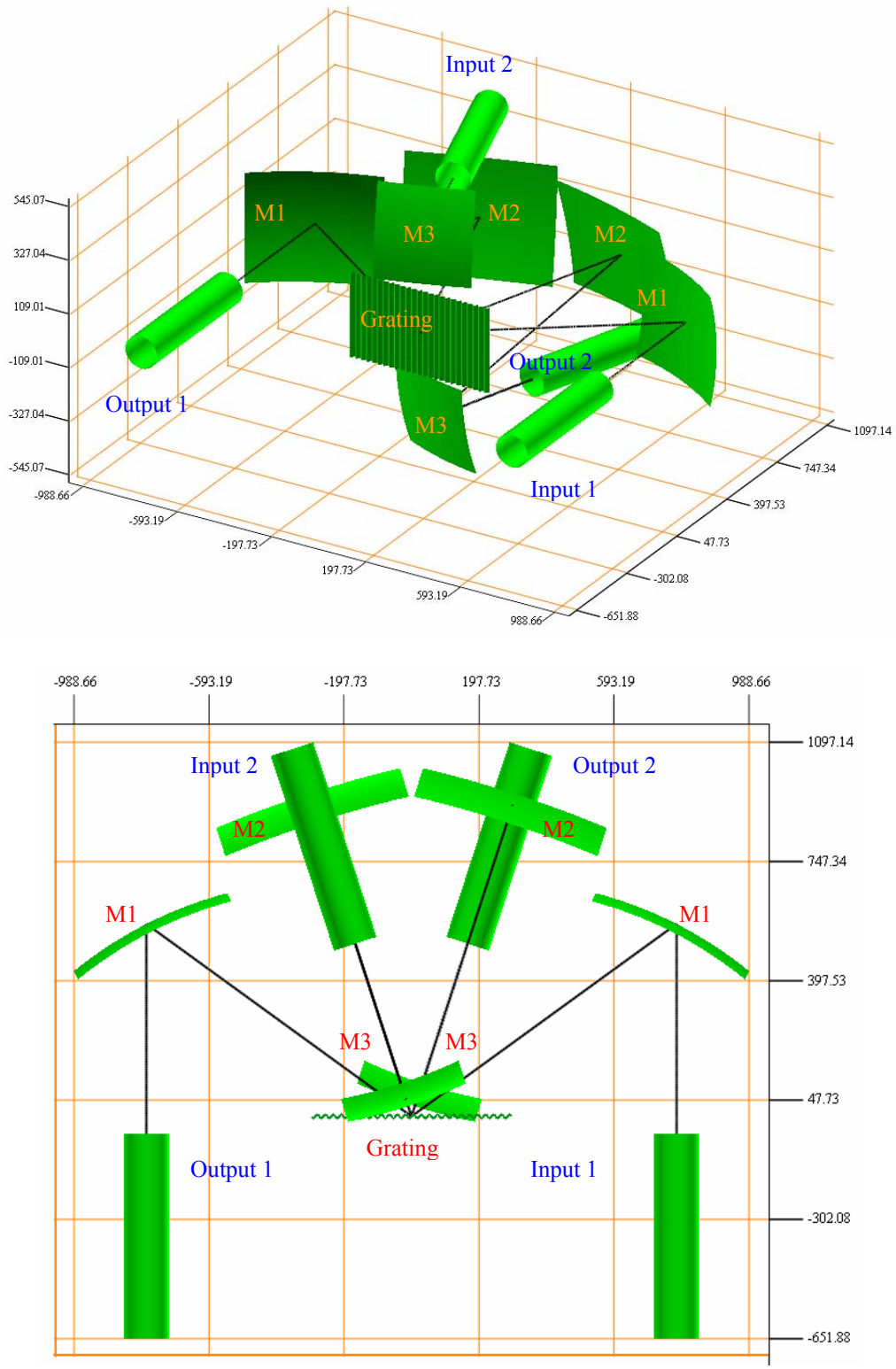

Fig. 11. Design of quasi-optical 11.4 GHz 3-dB hybrid: 3D and top views.

3d. Conceptual design for a 34-GHz magic-Y to be tested with the Omega-P magnicon

In Section 7, Phase II goals and plans for building, testing, and evaluating the magic-Y concept will be outlined. The device to be built is to be tested at pulsed power levels up to 25 MW, as derived from the Omega-P 34-GHz magnicon amplifier. The experimental arrangement would be similar to that shown in Fig. 12, which shows components as they will be installed in the Yale Beam Physics Laboratory adjacent to the magnicon; the particular installation shown in Fig. 12 is for a quasi-optical four-mirror passive pulse compressor now under development by Omega-P under a current Phase II SBIR grant. Existing components in each output arm of the magnicon to be used for testing the magic-Y include dual directional couplers, phase shifters, mode converters, and vacuum barrier windows. Two such outputs would be used, supplemented with transducers to generate Gaussian beams. Each transducer will be composed of an elliptical-cross-section waveguide to change the polarization direction of the TE_{11} mode, and a tapered horn for producing the TM_{11} admixture to the TE_{11} mode that will yield a resulting wave beam with a quasi-Gaussian transverse structure. One arm will contain a remotely-controlled motor-driven 0-180° phase shifter for switching the output beam from one channel to the other. The transducers are followed by a system of mirrors matching the wave beams to the grating. Two design arrangements are shown in Figs. 13 and Fig. 14; these differ in the character of wave beams at the magnicon output horns: if the beam at the horn aperture has a circular cross-section, two mirrors in each line are needed for beam matching to the grating (arrangement shown in Fig. 13); but if the beam at the horn aperture has the proper elliptical cross-section, one mirror is sufficient for matching (arrangement shown in Fig. 13). Clearly, efforts will be made to evolve an engineering design that conforms to the simpler arrangement of Fig. 14.

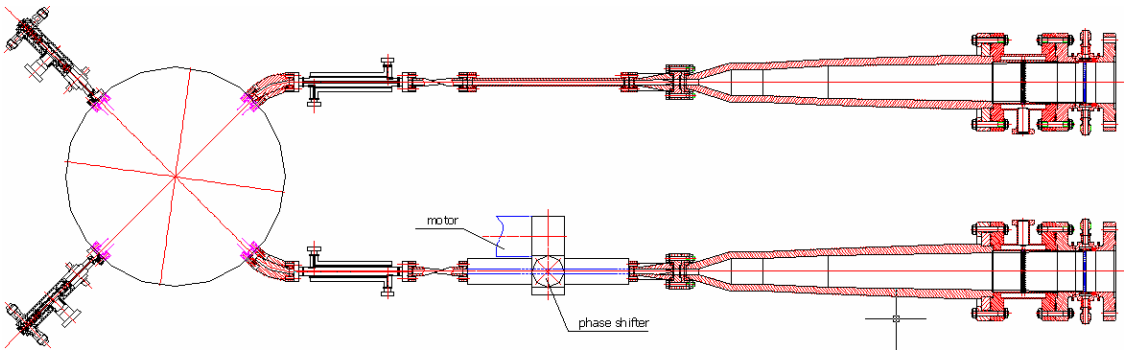

Fig. 12. Top view of the 34 GHz magnicon producing two Gaussian beams to feed the Magic Y. One of the wavguide feed arms includes a remote-controlled phase shifter.

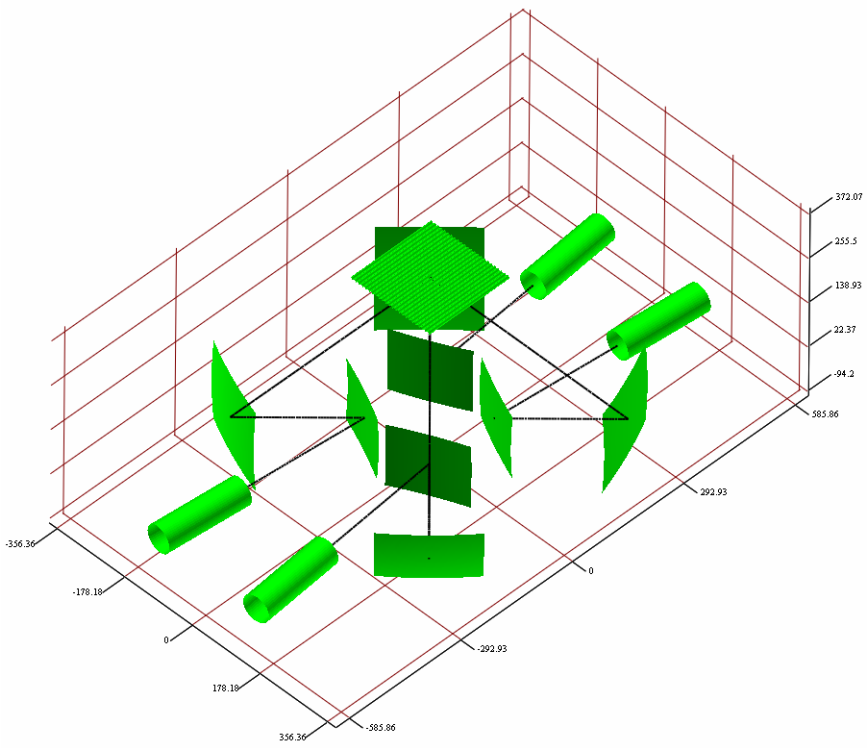

Fig. 13. One concept for the set-up for testing the 34 GHz magic-Y at high power. Each circular cross-section input beam is matched to the diffraction grating using two mirrors.

Parameters of the matching mirrors for the set-up shown in Fig. 13 are given in Tables V-VII.

Table V. Parameters of mirrors.

element	size (mm^2)	radii of curvature (mm^2)
M1	170×160	1268×938
M2	205×208	1250×1129
grating	212×212	∞×∞

The sinusoidal grating corrugation has a period of 8.747 mm and an amplitude of 1.86 mm.

Table VI. Distances between centers of objects.

element 1	element 2	distance (mm)
waveguide	M1	300
M1	M2	250
M2	grating	524

Table VII. Angles.

element 1	element 2	element 3	angle (deg)
waveguide	M1	M2	40
M1	M2	grating	45

The angle between horns is 10 degrees. Each horn axis is inclined at an angle of 5 deg with one of the main planes of symmetry.

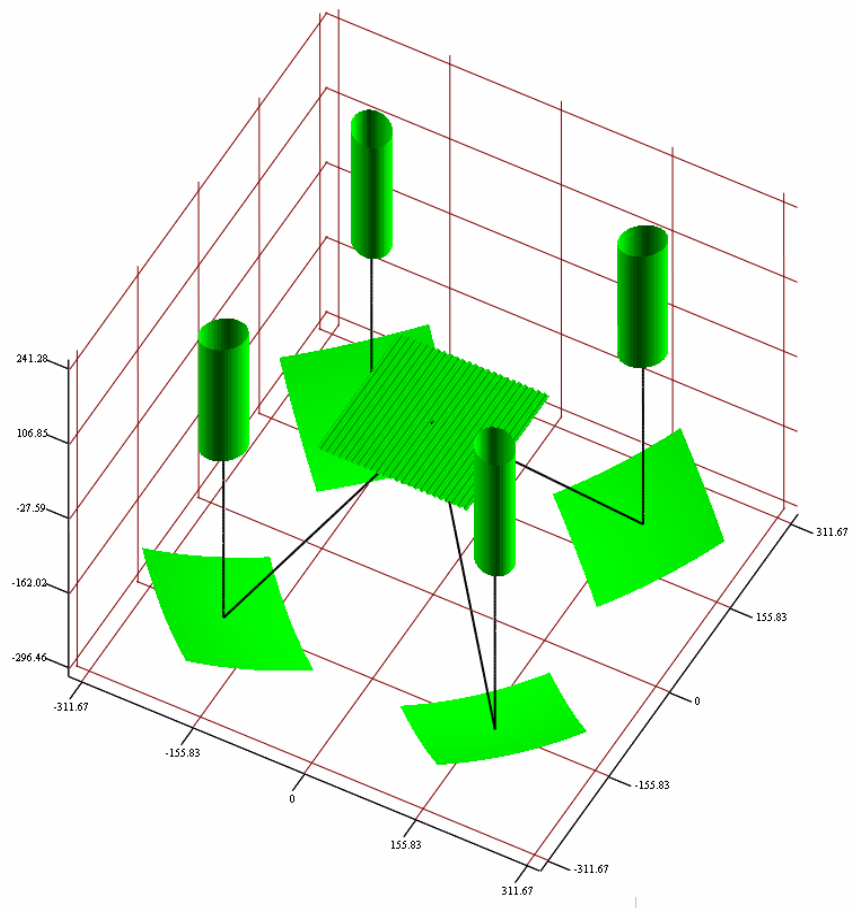

Fig. 14. A second (obviously preferred) concept for the set-up to test the 34 GHz Magic Y at high power, when each elliptic-cross-section horn is matched to the diffraction grating using one mirror.

Parameters of horns and matching mirrors are presented in Table VIII for the set-up diagrammed in Fig. 14.

Table VIII. Parameters of horns and mirrors for set-up shown in Fig. 13.

element	sizes (mm^2)	radii of curvature (mm^2)
horn	63.5×50.9	-
M1	177×192	590×556
grating	212×212	∞×∞

The grating sinusoidal corrugation has an amplitude 1.86 mm and a period 8.747 mm. The beam angle of incidence to the grating is 45 degrees. The angle of incidence of the beam to each focusing mirror is 22.5 degrees. The distance between the horn and the focusing mirror is 310 mm, while the distance between centers of the focusing mirror and the grating is 380 mm.

As will be described in Section 7, efforts during Phase II will be directed towards engineering design, fabrication, testing and evaluation of the conceptual set-up shown in Fig. 14.

References

1. Wilson, P. B., "Scaling linear colliders to 5 TeV and above," Stanford, CA, SLAC Rep. SLAC-PUB-7449, Apr. 1997.
2. Nezhevenko, O., in Proc. of 1997 Particle Accelerator Conference, Vancouver, Canada, (IEEE, Piscataway, NJ, 1997), 3013–3014.
3. Laurent, L., Scheitrum, G., Vlieks, A. et al., *RF Breakdown Experiments at SLAC*, in High Energy Density Microwaves, edited by Robert M. Phillips, AIP Conference Proceeding 474 (New York, American Institute of Physics, 1998), 261–278.
4. Braun, H., Luong, M., Wilson, I., Wuensch, W., *A very High Gradient Test of a 30 GHz Single Cell Resonant Cavity* CERN/PS 2000-045 (RF).
5. Braun, H., Dobert, S., Syrachev, I., Taborelli, M., Wilson, I., Wuensch, W., Technical Report CLIC Note No. 535, CERN, PS Division (2002).
6. Pritzkau, D. P., Siemann, R. H., *Experimental study of rf pulsed heating on oxygen free electronic copper,* Phys. Rev. Special Topics – Accelerators and Beams, 5, 112002 (2002).
7. Dolgashev, V., Tantawi, S., *Effect of RF Parameters on Breakdown Limits in High-Vacuum X-Band Structures,* Proc. RF-2003, Coolfont Resort.
8. Nezhevenko, O.A., LaPointe, M.A., Yakovlev, V.P., Hirshfield, J.L., *34 GHz, 45 MW pulsed magnicon: first results*, Proc. RF-2003, Coolfont Resort.
9. Petelin, M.I., Caryotakis, G., Tolkachev, A.A. et al., *Quasi-Optical Components for MMW Fed Radars and Particle Accelerator.* High Energy Density Microwaves, AIP Conference Proc. 474, Pajaro Dunes, California, Oct. 1998, Ed. Robert M. Phillips, Woodbury, New York , pp. 304-315.
10. Petit, R. (ed.), Electromagnetic Theory of Gratings, Berlin-Heidelberg-New York: Springer-Verlag, 1980.
11. Mizuno, H., Otake, Y.: "A New RF Power Distribution System for X-band Linac Equivalent to an RF Pulse Compression Scheme of Factor 2n," Proc. LINAC94, 1994.
12. *Quasi-optical accelerating structure for electron-positron collider*, Omega-P Phase-I report, DoE SBIR grant 2002.
13. Wilson, P. B., in Proccedings of the ITP Conference on Future High Energy Colliders, University of California, Santa Barbara, 1996.
14. *High power microwave pulse compressors,* Omega-P Phase-I report, DoE SBIR grant, 2002.
15. Vikharev, A.L., Danilov, Yu.Yu., Gorbachev, A.M., Kuzikov, S.V., Koshurinov, Yu.I., Paveliev, V.G., Petelin, M.I., Hirshfield, J.L., *Quasi-Optical Microwave Pulse Compressor at 34 GHz*, Proc. 8th Advanced Accelerator Concept Workshop, Oxnard, CA, June 20, 2002.
16. Petelin, M.I., *Quasi-Optics in High-Power Millimeter-Wave systems*, Proc. RF-2003, Coolfont Resort.